Powder Technology 443 (2024) 119969

Contents lists available at ScienceDirect

Powder Technology

journal homepage: www.journals.elsevier.com/powder-technology

Novel insights into sylvite flotation modulated by exposing facets

Yuan Yuan [a,b,c], Weiquan Zhan [a,d], Alejandro Lopéz Valdivieso [e], Songliang Ma [f], Yang Tian [b], Hao Yi [a], Guangfeng Dong [f], Shaoxian Song [e,*], Luis A. Cisternas [g], Feifei Jia [b,*]

[a] Key Laboratory of Green Utilization of Critical Non-metallic Mineral Resources of Ministry of Education, Wuhan 430070, Hubei, China
[b] School of Resources and Environmental Engineering, Wuhan University of Technology, Wuhan 430070, Hubei, China
[c] Doctorado Institucional de Ingeniería y Ciencia de Materiales, Universidad Autónoma de San Luis Potosí, Av. Sierra Leona 530, San Luis Potosí 78210, Mexico
[d] Instituto de Física, Universidad Autónoma de San Luis Potosí, Av. Manuel Nava 6, Zona Universitaria, San Luis Potosí 78290, Mexico
[e] Instituto de Metalurgia, Universidad Autónoma de San Luis Potosí, Av. Sierra Leona 550, San Luis Potosí 78210, Mexico
[f] SDIC Xinjiang Luobupo Potash Co., LTD, Hami, Xinjiang 839000, China
[g] Departamento de Ingeniería Química y Procesos de Minerales, Universidad de Antofagasta, Antofagasta, Chile

HIGHLIGHTS

- Sylvite flotation behaviors connected with exposing facets were firstly investigated.
- Sylvite with (002) facet possessed higher flotation recovery than that with (222) facet.
- Stronger adhesion of bubbles on (002) facet facilitated flotation recovery.
- Interaction between exposing facets and collector was electrostatic adsorption.
- Negative surficial potential of (200) facet was originated from edges with hanging Cl bonds during its layered growth.

GRAPHICAL ABSTRACT

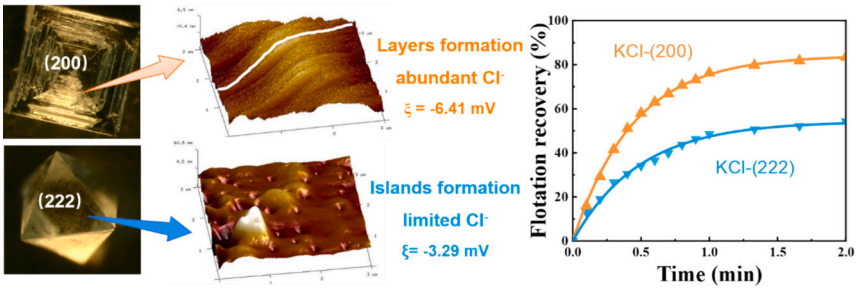

ARTICLE INFO

Keywords:
Octahedron KCl
Lead ions
Exposing facets
Surficial properties
Flotation

ABSTRACT

Sylvite (KCl) is a classical soluble mineral with high solubility, endowing the possibility to precisely adjust its surficial structure for flotation recovery. In this work, efforts have been originally made to study flotation behaviors of KCl with (200) and (222) exposing facets. KCl(200) crystals had a higher recovery than that of KCl (222) with octadecylamine hydrochloride (ODA). FTIR and XPS results indicated that interaction force between KCl and ODA was not chemical absorption. Zeta potential results further implied the mechanism that the ODA reacted with KCl by static force and KCl(200) possessed a lower potential than KCl(222) and thus facilitated the flotation process. 2D as well as 3D AFM results provided microscopic details of perfect cubic KCl(200) and octahedron KCl(222) samples where layered growing method of former samples exhibited more edges with hanging Cl bonds, leading to its more negative surficial potential and less hydrophilic property, enhancing flotation recovery. Moreover, adhesion & adsorption force further illustrated that KCl(200) obtained a stronger interaction with bubbles, in coincidence with its better flotation recovery. KCl crystals with (200) exposing faces promoted flotation in comparison with crystal with (222) faces, offering strategy to reserve (200) faces for designing KCl crystals with high recovery.

* Corresponding authors.
E-mail addresses: ssx851215@whut.edu.cn (S. Song), feifeijia@whut.edu.cn (F. Jia).

https://doi.org/10.1016/j.powtec.2024.119969
Received 25 March 2024; Received in revised form 29 April 2024; Accepted 3 June 2024
Available online 4 June 2024

1. Introduction

KCl, one of key water-soluble minerals [1], was mined and processed to provide potassium compounds for agricultural industry [2] and other chemicals like medicine [3], battery [4], ceramics [5], plastics [6], etc. Since the 1940s, the majority of potash ore was extracted through flotation in potash industry [7–9]. As the increased demand of potash elements and lower grade of potassium ore, potassium supply is in urgent requirement all over the world [10,11]. Hence, further improving flotation recovery is critical for optimization of flotation system in industry.

Adjusting hydrophobicity of crystal surfaces and the selectivity of bubble and crystal interaction during flotation process were main way to improve recovery of potash ores [12–14]. For decades, precursors focused on developing various surfactants (called as collectors) comprising of hydrophilic group and hydrophobic chain in difference of flotation selectivity and capability, such as, primary alkylamines (R-NH_2) [15] in early stages, sodium alkylamines (R-SO_3Na) [16], sodium alkylsulfates (R-OSO_3Na) [17], and fatty acids (R-COOH) [18]. Despite abundant types of collectors were applied in the industry, flotation recovery still requires further improvement.

Considering that most minerals are crystals whose one typical feature is the well-defined notion of standard repeating units with discernible crystallographic plane, crystal samples exhibit different physical and chemical properties with various exposing faces [19–21]. For instance, one extreme but common example is two-dimensional crystal materials type showing obvious anisotropy like molybdenite [22,23], mica [24], talc [25] and highly oriented pyrolytic graphite (HOPG) [26] that can be easily exfoliated to layers along basal (001) plane but difficult to destroy from the other vertical (010) direction, where the latter plane with hanging unsaturated bonds tends to be more active to react with collectors and bubbles during flotation process [27–29]. On behalf of natural KCl crystals which belongs to typical face-centered-cubic (FCC) type, the most common two structures with single-type exposing faces are i. six square (200) faces composing one cubic structure and ii. eight triangle (222) faces forming an octahedron structure [30,31]. Moreover, thanks to KCl crystals' good solubility which highly relies on solution conditions [32,33], samples with various exposing faces can be obtained during the crystallization process by well-designed strategies. It is likely that the uncommon exposing facets may bring new possibility or show disadvantages, which should be well researched for reaching an ideal flotation recovery. Hitherto, few studies investigated the work about improving floatation of KCl by modulating exposing facets.

During the industrial production, the most used method to recover potassium is by cold decomposition followed with froth flotation using ODA (not only for recovery of KCl but also for restrain of tail mineral NaCl) as collector [34,35]. Here, KCl crystals with only one type of exposing faces as (200) and (222) were obtained where the surfaces details were shown by atomic force microscope (AFM) to research their growing mechanisms. Flotation performances of two types of KCl samples as well as their corresponding interaction with ODA were well studied by fourier transform infrared spectroscopy (FTIR) and X-ray photoelectron spectroscopy (XPS). Besides, the induction time test and adhesion & adsorption force tests were conducted to further study the interaction behaviors during flotation process. The related mechanism of different flotation recovery with two types of KCl crystals were researched.

2. Materials and methods

2.1. Reagents

Analytical pure grade KCl and hydrochloric acid (HCl) reagents were purchased from Sinopharm Chemical Reagent Co., Ltd., China, while pure lead chloride ($PbCl_2$) and octadecylamine hydrochloride reagents from Aladdin Pharmacy company. During all experiments, pure deionized water (Millipore SAS, France) with a resistivity of 18.2 MΩ cm and KCl were mixed to prepare the saturated KCl solution.

2.2. Preparation of KCl samples with various exposing facets

The growing process of crystals highly depends on the solution condition according to the solubility curve. For salt crystallization, the main variations include the concentration of composing ions, temperature range and evaporation area (liquid-gas area), and also the additives. Here, based on properties of KCl salt, mild crystallization reaction and addition of Pb ions methods were chosen to grow KCl crystals with (200) exposing facets and (222) facets, respectively. For flotation experiments, the samples were sieved to gather same size range between 178 and 250 μm to exclude the impactor of particle size. The detailed preparation methods were described as below.

2.2.1. Preparation of KCl crystals with (200) exposing facets

It's known the fact that crystal habit of KCl is cubic with six square (200) faces. However, perfect cubic with sharp corners only appears under gentle growing environment due to its easily crystallization with slight decline of temperature as well as evaporation of water. Hence, a mild isothermal evaporation method was performed to prepare the perfect cubic KCl crystal. In a typical experiment, saturated KCl solution was poured into a petri dish with diameter of 15 cm for 48 h with stirring speed at 300 rpm to grow even cubic KCl crystals. For bigger cubic crystals the evaporation period was extended to one week and perfectly formed KCl samples were carefully moved to a filter paper for quick drying to maintain the flat and immaculate surface for delicate tests like AFM.

2.2.2. Preparation of KCl crystals with (222) exposing facets

According to previous research by L. Pastero, R [36], ratio of exposing facets including (200) and (222) of KCl crystals highly depends on the additive of $PbCl_2$. The increasing amount of lead ions would promote the proportion of (222) face of KCl crystal. Thus, for pure (222) exposing face KCl crystals with octahedron morphology, ratio at 1:500 in weight of pure $PbCl_2$ in grams and saturate KCl solution in volume was prepared and ultrasonic process with intensity at 200 W for 20 min was performed to ensure the well mixture of composing substances. Then the solution was poured into a petri-dish for slowly evaporation & crystallization reaction for a certain period, based on the requirement of crystal size. After that, the well grown crystals were selected by a dropper and dewatered by filter paper immediately in order to keep perfect crystals unblemished for surficial observations as well as avoiding the further growth. Finally, Pb-KCl samples were kept in an oven at 45 °C overnight to dry up for next measurements to minimize the moisture absorption due to the high hydrophilia of KCl salt.

2.3. Characterization

For observation of crystals, a stereoscopic was performed due to their large scale of size with nearly perfect morphology. With smaller size crystals, scanning electron microscope (SEM, Phenom ProX G6, Netherlands) was used for detailed observation of intact octahedron and cubic KCl crystal surfaces. Atomic force microscope (AFM, Bruker MM8, German) with ScanAsyst Air mode equipped with Air tip helped to reveal the surficial morphologies of grown perfect cubic and octahedron KCl crystals and the results were analyzed by Bruker Nanoscope Analysis 1.4 software. X-ray photoelectron spectroscopy (XPS, Thermo Scientific ESCALAB Xi+, America) and X-ray diffraction (XRD, D8 Advance, Germany) tests with Cu-Kα sealed tube were applied to study the crystalline structure of KCl crystals and the latter also helped to understand the exposing face differences between variously-shaped KCl samples. Besides, FTIR (Nicolet 6700, UK) along with Zeta potential test (Malven, UK) were conducted to study the interaction between the collector ODA

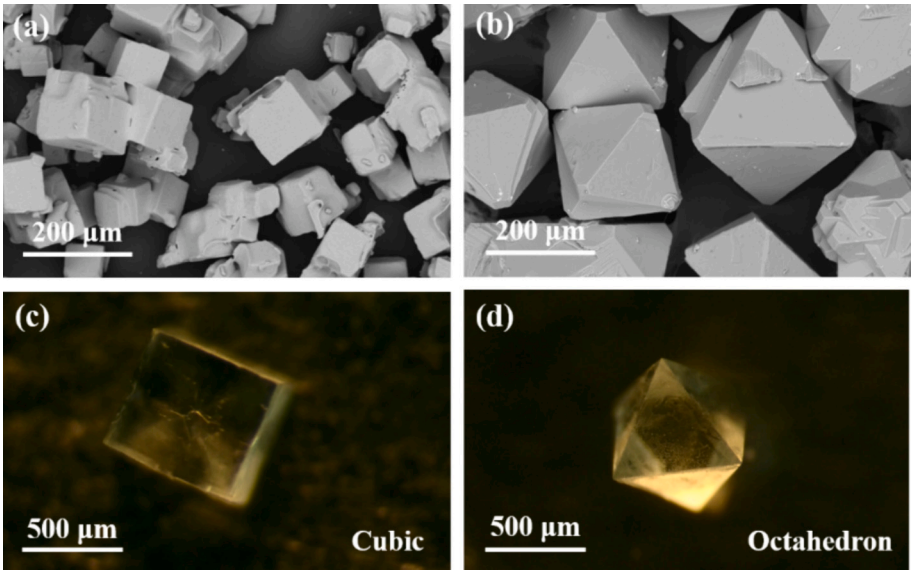

Fig. 1. SEM results of cubic (a) and octahedron (b) crystals, and their corresponding stereoscope results.

and mineral sample KCl. Especially for the zeta potential test, KCl samples were ground to obtain powder with particle size less than 5 μm to suspend in saturated KCl solution. For zeta potential tests related with ODA, the concentration was set to be the same as flotation process as 60 g/t in saturate KCl solution. The mixture was conditioned for 20 min and then measured for 6 times to yield the average zeta potential information.

2.4. Floatation experiments

To study how potassium chloride with (200) exposing face and (222) exposing face would affect the recovery process with ODA as collector reagent, flotation experiments of cubic- and octahedron-shaped KCl crystals with same size range of 178–250 μm were conducted in a flotation cell with capacity of 60 mL and the pulp concentration was set to be 25%, under ambient temperature around 25 °C. *prior* to the experiment, the collector ODA reagent was prepared by mixing 2 mL pure HCl into 99 mL octadecylamine solution. The mixture was heat up to 80 °C until clear to maintain its high activity each time before flotation. During a standard floatation process. 15 g of grown KCl crystal particles was added into 60 mL of saturated KCl solution and conditioned for 3 min. Then, 45 μL of transparent ODA was added with mixing for another 2 min. Afterwards, bubbles were performed at flow rate of 0.1 L/h with air as source for 2 min. Flotation process was carried out then for two minute to get the flotation kinetics date. All samples were immediately filtered and transferred to an oven at 45 °C to dry up to avoid further crystallization with remnant saturated KCl solution on surface of crystals. The flotation kinetics was described by classical flotation kinetics

$$\varepsilon = \varepsilon_{\infty}[1 - exp(-\mathrm{kt})] \quad (1)$$

where ε and ε_{∞} were real and theoretical recovery, %; k was flotation rate, min^{-1}, t was the flotation time, min.

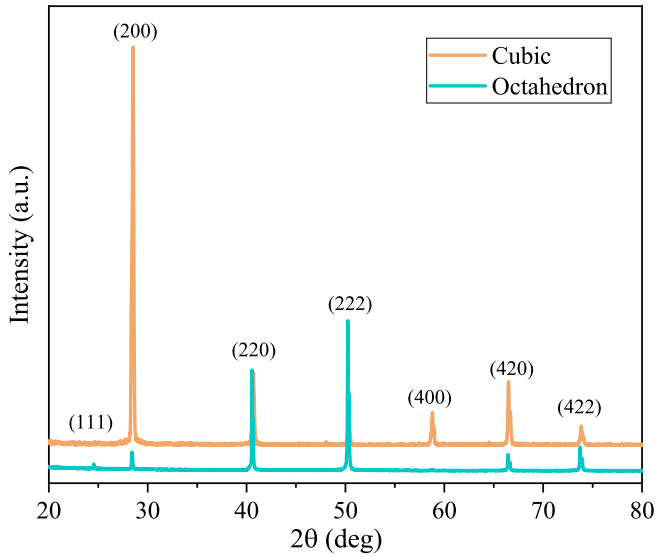

Fig. 2. XRD results of cubic and octahedron crystals.

2.5. Adhesion & adsorption force test

During flotation process, another key parameter is the interaction force between minerals and bubbles. Here, the adhesion & adsorption force tests were conducted by a surface tension measurement apparatus (Powereach JK99M2, China). Notably, the unstable bubble under solution hindered the accuracy of interaction test but liquid drop helped to get a better understanding. The interaction law between particles & bubble could be easily obtained by reversing the rule of particles & flotation solution. During the test, a ring tip with a droplet with ~50 μL of saturated potassium chloride solution was hanged where its weight was evaluated by the digital sensor of instrument. Then, the cubic or octahedron samples were firstly immersed in saturated KCl solution with 60 g/t addition of collector ODA for 10 min in order to realize the same situation during flotation process. Then the samples were dried at 45 °C for 4 h to dry up and placed on the surface of a glass slide with a relatively smooth surface, which was later put on the instrument platform to move forward the droplet with velocity at 0.01 mm/s to ensure the accuracy of this test. The distance between droplet and particles was well designed in order to make sure about the contact. Afterwards, the sensed real-time mass changes were recorded and adhesion & adsorption force data could be read by analysis of the curve.

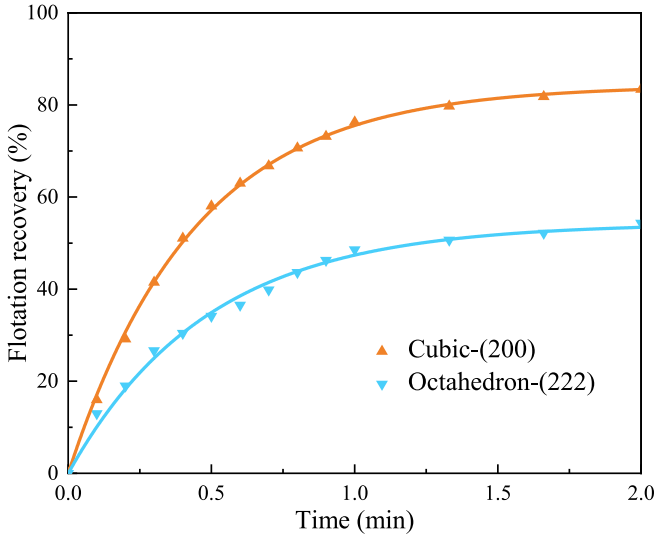

Fig. 3. Flotation kinetics results of KCl(200) and KCl(222) crystals using ODA.

Table 1
Kinetic parameters for flotation kinetics of classical first-order model.

	Classical first-order model		
Samples	ε_∞ (%)	k_1 (min^{-1})	R^2
Cubic	84.24	2.27	0.999
Octahedron	54.31	2.06	0.994

3. Results and discussion

3.1. Morphology characterization

By cooling and lead addition methods, two types of KCl crystals were successfully prepared and their morphology information was studied by SEM and stereoscopy, as shown in Fig. 1. It's clear that cubic morphology appeared during cooling method, while octahedron morphologies showed up with existence of small amount of lead ions. The uneven size distribution was due to the easily crystallization of KCl in solution but sieves helped to narrow samples to proper size ranges for other tests. In Fig. 1c and d, the cubic and octahedron samples shared nearly perfect shapes with only one type smooth surfaces, indicating their high crystallinity which was further researched by XRD test in the following results.

3.2. Crystal structure

As one of the most important features of crystals, the crystalline structure of KCl samples with cubic and octahedron shapes were studied here. Firstly, the XRD test was performed to cubic and octahedron and corresponding results were displayed in Fig. 2. Peaks at around 24.5°, 28.5°, 40.6°, 50.2°, 58.8°, 66.5° and 73.8° were ascribed to (111), (200), (220), (222), (400), (420) and (422) faces of KCl crystals, which were in high agreement with the PDF#73–0306 data of KCl [37,38]. The high and narrow peaks demonstrated that both two samples pertained high purity of KCl crystal while the cubic sample showed high intensity of (200) face and octahedron sample of (222) face, indicating their different main exposing faces. Besides, the addition of lead ions did not change the structure of KCl crystal but only the exposing face, giving the chance to study the influence of KCl exposing face on its recovery possibility as discussed in the coming part of this work.

3.3. Flotation affected by crystal facets

The flotation experiments of two types of crystals with (200) and (222) exposing faces with size range at 178–250 μm using ODA as collector were conducted, and the flotation kinetics results were shown as Fig. 3. Both flotation recovery in the process were highly coincident with classical first-order model, as listed in Table 1. The flotation rate of KCl (200) was higher than that of KCl(222). The KCl(200) samples achieved a recovery at 83.35%, while recovery of KCl(222) was about 53.42%, demonstrating a better interaction between cubic KCl crystals with bubbles under collector as ODA.

3.4. Interaction between KCl crystal and collector

In most cases, the minerals would absorb collectors to reach a hydrophobic stage so as to attach to bubbles for being floated. The good flotation behaviors of two samples implied the possible interaction between KCl particles and ODA. Here, FTIR tests was used to study if ODA was absorbed on KCl crystals. From Fig. 4, it was clear that before flotation, both KCl(200) and KCl(222) samples showed peaks at 1638.00 and 1114.00 cm^{-1}, belonging to KCl [39,40]. After reaction, there were new peaks at 2917.77, 2850.27, 1473.35 and 719.32 cm^{-1} on KCl(200) and 2919.70, 2852.20, 1473.35 and 875.53 cm^{-1} on KCl(222) samples, which all belong to ODA, demonstrating the successful adsorption of ODA on KCl samples [41,42]. However, the interaction type remained unclear which needed further investigation by following XPS tests in Fig. 5.

To further figure out the interaction details between KCl crystals and collector ODA, binding energy information of different elements of KCl (222) before and after flotation was tested by XPS and the related results were displayed in Fig. 5. In the survey map, Pb, K and Cl element narrow

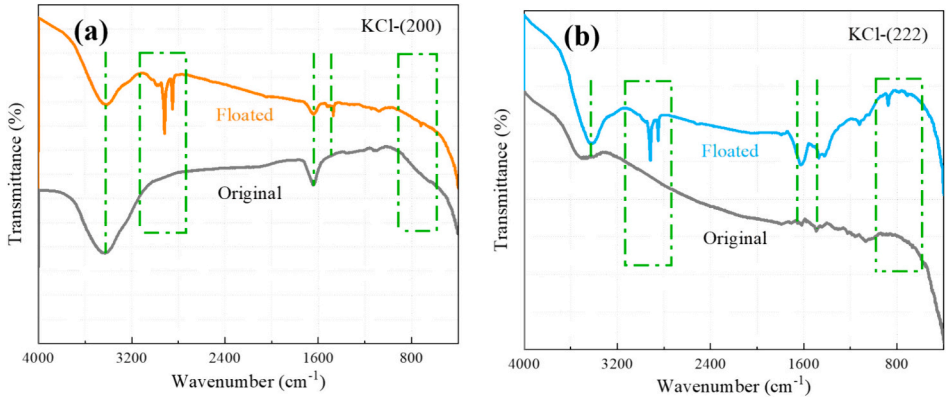

Fig. 4. FTIR results of KCl(200) and KCl(222) crystals before and after flotation, respectively.

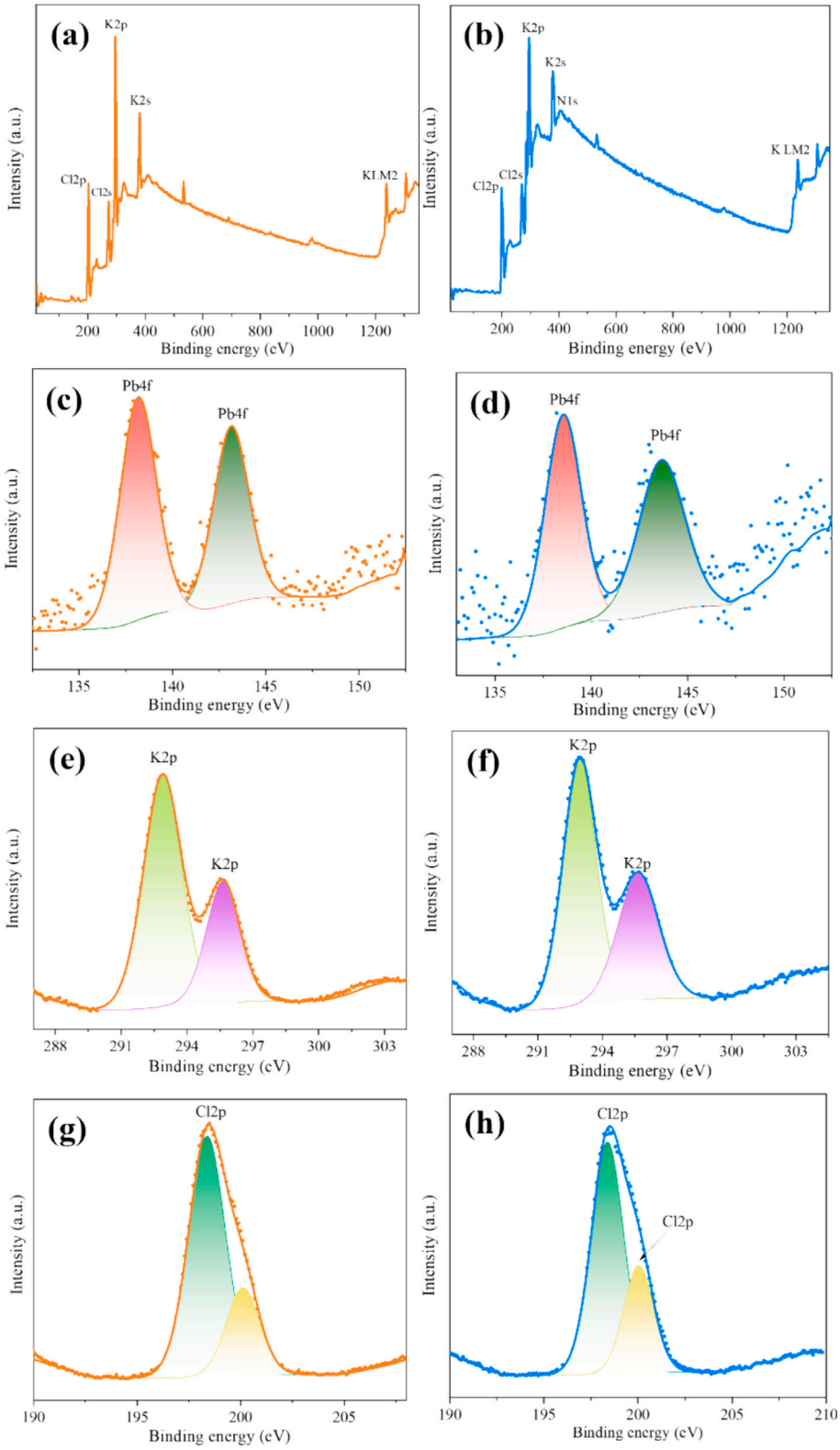

Fig. 5. XPS spectra of KCl(222) samples before: (a) survey, (c) Pb 4f, (e) K 2p, (g) Cl 2p and after flotation: (b) survey, (d) Pb 4f, (f) K 2p, (h) Cl 2p.

map of original KCl(222) sample were shown in left four maps in Fig. 5a, c, e and g, respectively and their corresponding maps after flotation in right maps of Fig. 5b, d, f and h. Notably, the Pb 4f peaks at 138.64 eV and 143.65 eV in Fig. 5c belonged to KPb_2Cl_5 [43], it could be ascribed to the minor addition of Pb ions inserting in the crystal structure of KCl (222). By comparing the peaks between left and right, the binding energy difference could be clearly seen that no movement occurred in Pb 4f, K 2p and Cl 2p spectra, indicating that none of new chemical bonds appeared. As a consequence, the force between KCl(222) and ODA do not belong to chemical adsorption but probably only physical reaction that needed other investigation.

The above FTIR and XPS results suggested that the ODA's adsorption

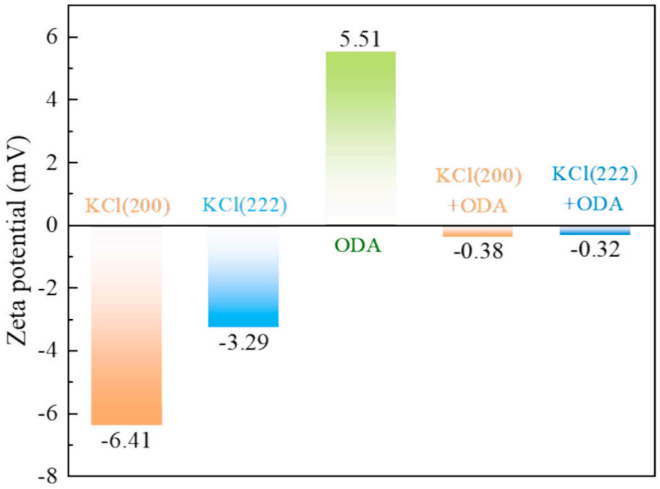

Fig. 6. Zeta potential results of KCl(200), KCl(222) crystals before and after reacting with ODA, and of ODA in saturate KCl solution.

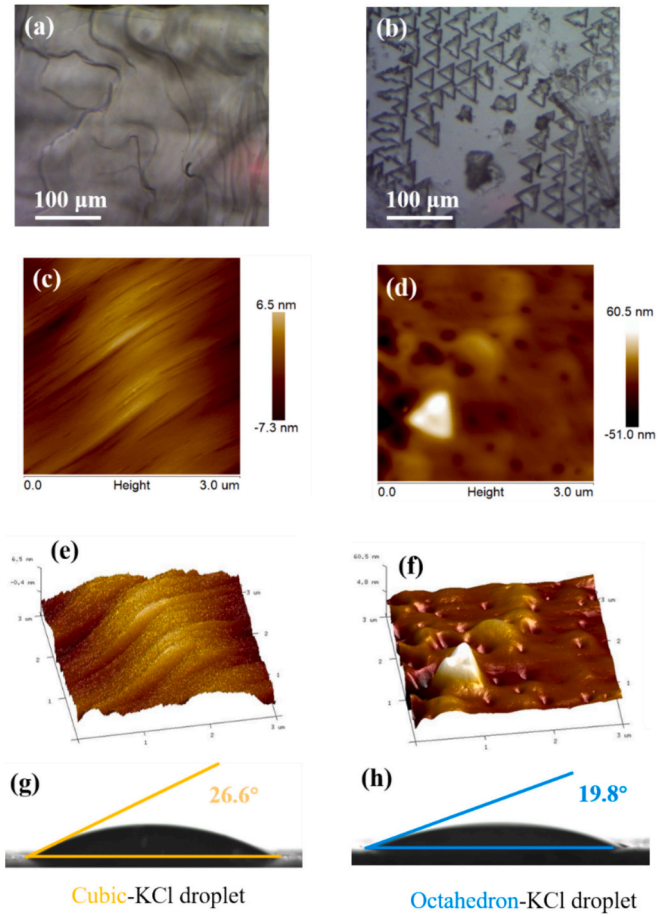

Fig. 7. (a, b) Micrographs, (c, d) two dimensional & (e, f) three dimensional AFM and (g, h) contact angle results of KCl(200), KCl(222) crystals, respectively.

on KCl could be ascribed to non-chemical force. To reveal the mechanism, zeta potential of KCl(200), KCl(222) before and after reacting with ODA were tested and related results were displayed in Fig. 6. It's known the fact that ODA is a cationic collector with positive charge which was also demonstrated here. In Fig. 6, before reaction, KCl(222) and KCl (200) possessed −3.29 mV and − 6.41 mV, respectively. According to previous work [44], similar to LiCl with negative zeta potential, the hydration energy of K ion is higher than that of Cl ion which promotes the dissolve of K ions into solution instead of Cl ions on surface of KCl crystal structure, resulting in the more left Cl^- with negative charge of KCl crystals as demonstrated in Fig. 6. The different zeta potential of these two samples would be well explained in later discussion. Anyway, as a result, the more negative zeta potential of KCl(200) indicated the better static interaction with cation collector ODA (5.51 mV) than that of KCl(222) crystal during flotation, well explaining the different flotation behaviors. Afterwards, cubic and octahedron samples achieved an increased zeta potential to −0.38 and − 0.32 mV, close to zero, suggesting the possible physical static force between KCl and ODA which was in coincidence with previous conclusion [45].

As mentioned above, flotation happens by the selected adsorption by collectors on minerals surfaces to reach a hydrophobic condition in order to interact with bubbles. As a consequence, the surficial properties of minerals show a vital role in this reaction. AFM, as a powerful atomic level method to reveal the surficial morphology, was adopted to help understand the properties of KCl(200) and KCl(222) crystals whose slowly grown perfect samples pertained flat surfaces. Shown in Fig. 7a and b were the surficial morphology of cubic and octahedron from the microscope equipped with AFM where the former sample had a clean and flatten surface but latter with several triangle islands. The KCl(200) sample with cubic structure was grown by mild evaporation which allowed a slow and steady growth to exhibit a nearly perfect cubic shape with flat surfaces, in coincidence with FCC crystal structure. However, the KCl(222) sample with octahedron shape was grown by a different way from cubic structure that on each (222) triangle face, the extra ions firstly formed a small triangle island and then bigger. Those islands finally successfully grow to connect with each other to form another layer, thus to realize a bigger octahedron crystal. More detailed surficial information was displayed in Fig. 7c, e by two-dimensional results andtheir corresponding three-dimensional results from AFM tests in Fig. 7d and f. It's worth noting that the AFM results were corresponding to their microscope results where a flat and clean spot was chosen to endow the engagement of the tip. It's clear that on the surface of KCl (200), there were many stages composing of layers with large amount of exposing "edges", indicating the growth of (200) faces were by layers and the possible plentiful hanging Cl^- on the edges that resulted in its lower zeta potential value. For KCl(222) sample, there was one triangle island in Fig. 7d and f, in consistent with the microscope result in Fig. 7b. The uneven distribution of smaller punctate hills on surface might be the undergrown triangle islands. One other fact that Cl ion possessed higher binding energy with Pb ion than that with K ion, further strengthened the ability of KCl(222) to confine Cl ions inside the structure rather than dissolve into bulk saline. Compared with layered surface with abundant exposing edges on KCl(200) surface, the island-formation growth method hindered the exposing of edges as well as hanging Cl^- and lead to the relatively more positive surficial charge than KCl(200), as demonstrated by previous zeta potential results. In addition, the surficial properties also played a vital role in minerals' hydrophilia which further influenced the interaction with bubbles during flotation process. Contact angle results of saturated KCl solution on KCl(200) and KCl(222) in Fig. 7g and h suggested that the former cubic sample had a less hydrophily which could be ascribed to its more exposing of Cl^- with lower hydration energy than K^+. The less hydrophilic KCl(200) facilitated the adsorption of cubic KCl crystals with bubbles to obtain a better flotation recovery as described above. In consideration of the morphology and shape features of KCl(222) crystal, it's reasonable that one other disadvantage of its low floatability was that the unstable gravity center of octahedron structure hindered the attachment with bubbles during turbulent solution environment of flotation process.

As one result from surficial properties, adhesion & adsorption forces between mineral particles and collectors are thought to be another important test to unveil the flotation mechanism. Known as one typical hydrophilic mineral, KCl processed a relatively bubble-repelling

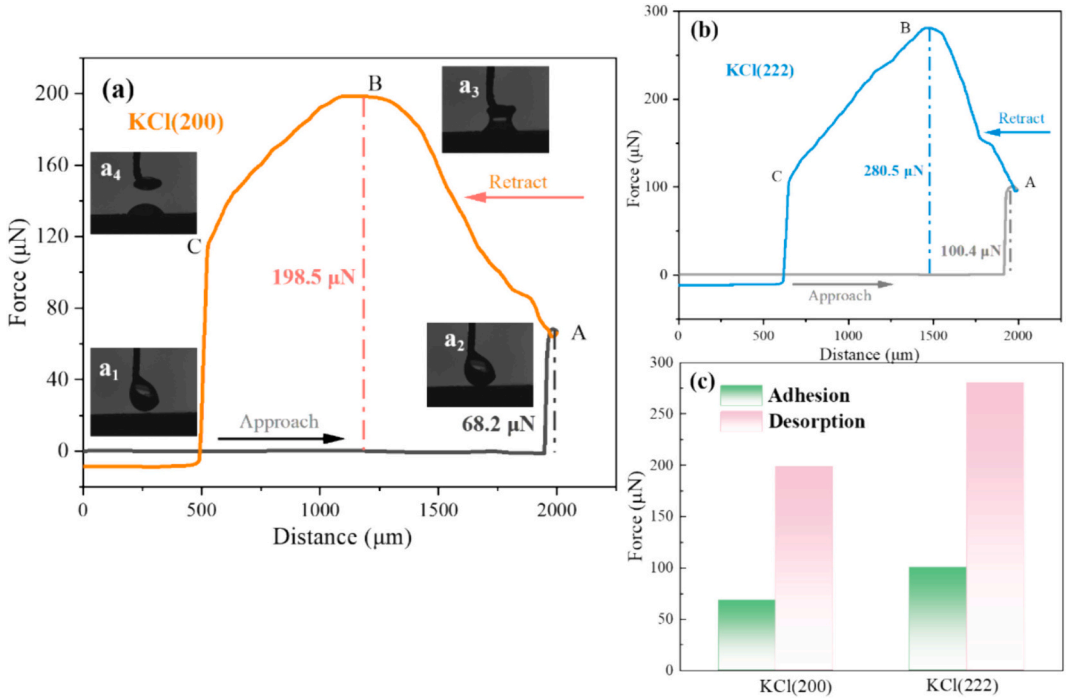

Fig. 8. Adhesion & adsorption force results of (a) KCl(200) and (b) KCl(222) crystals with saturated KCl drop, inserted in (a) were the photograph of (a_1) approaching, (a_2) contacting, (a_3) adhesion and (a_4) adsorption process, and (c) corresponding force information.

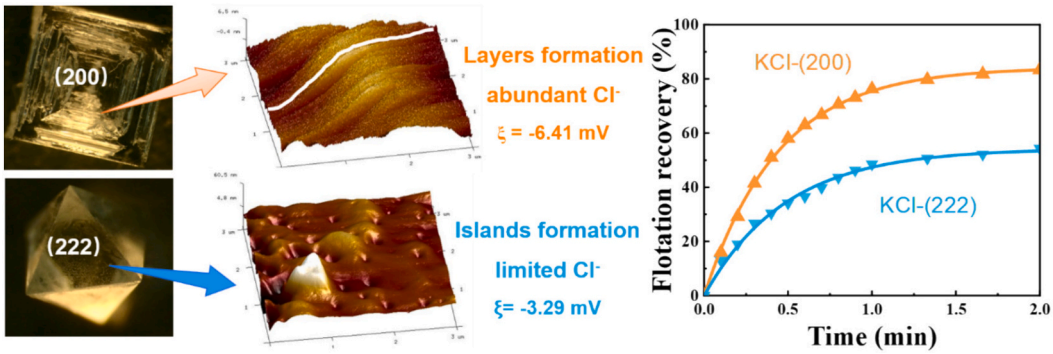

Fig. 9. Illustration of flotation behavior of KCl crystals with various exposing faces.

property. Here, the adhesion & adsorption forces between ODA-adsorbed KCl(222), KCl(200) samples with saturate KCl solution were studied to get a better understanding of the interaction behavior during flotation process, and the related results were displayed in Fig. 8 with a few typical records during the approaching & retracting process inserted in Fig. 8a. The real-time record of force revealed the adhesion force during the approach and retract procedure. It's clear that before contacting, the force was recorded to be a straight line without any change, until point A as shown in Fig. 8 (a_2), where a slight jump-into adhesion happened with a force at 68.0 μN. Afterwards, the liquid drop and sample KCl(200) platform moved together for a short time and then started the retract process. With the platform going down slowly, the adsorption occurred between the drop and sample, reaching a maximum adsorption force at 198.5 μN at point B. At last, the departure of drop from the sample occurred with the increase of distance at point C, the whole process ended with part of solution remaining on surface of sample which led to the remaining negative value instead of zero as shown in Fig. 8(a_4). Similarly, the adhesion and desorption force of sample KCl (222) in Fig. 8b were read as 100.4 μN and 280.5 μN, respectively. The stronger interaction force between KCl(222) with KCl saturated solution implied its weaker interaction with bubbles due to the difference between liquid and gas properties. Hence, the adhesion & adsorption force between KCl(222) and bubbles would be lower than that between KCl(200) and bubbles, giving another explanation of the worse flotation recovery of KCl(222) crystals.

3.5. *Illustration for flotation process*

All the results above suggested that the KCl(200) samples pertained a better flotation recovery compared with KCl(222) samples, the related mechanism has been well studied and the main concepts were illustrated in Fig. 9. It is shown that KCl(200) sample with cubic structure has 6 square (200) surfaces where the K and Cl ions in solution get to be attracted to stages of multilayers with abundant of edges and hanging unsaturated bonds. Nevertheless, KCl(222) crystal with octahedron structure contains 8 triangle (222) surfaces where new K and Cl ions form small triangle islands to help grow bigger octahedron structure. Its islands formation instead of layers piling up growing way indicated the integrality of KCl units with limited defects. The less hydrophily of Cl ions than K ions endows its higher possibility to stay in crystal structure

while hydrated K ions preferring to resolve in solution (saturated KCl solution, in this case). The more hanging Cl ions on surfaces of KCl(200) than KCl(222) crystals well explained its weaker hydrophily as well as lower surface charge that further facilitate its floatability by using ODA.

4. Conclusions

The KCl crystal with (200) and (222) exposing faces displayed various flotation recovery as 83.35% and 53.42%, respectively. The improved flotation ability of KCl(200) could be ascribed to the below mechanisms:

(1) By combining XRD and SEM results, it was concluded that KCl (200) samples was in cubic structure while KCl(222) samples with octahedron shape. FTIR result demonstrated the successfully adsorption of ODA on both KCl(200) and KCl(222) crystals after flotation, where XPS spectra helped to exclude the chemical interaction in between;
(2) Zeta potential tests demonstrated that KCl(200) crystals pertained a more negative zeta potential as −6.41 mV than that of KCl(222) as −3.29 mV, facilitating the stronger adsorption with cationic collector ODA with 5.51 mV surficial potential;
(3) The surfaces details obtained by AFM tests indicated that the growing method of KCl(200) crystals is by layers piling up to form stages with abundant edges and hanging Cl bonds, while KCl (222) was by formation of independent triangle islands with limited edges. The former sample with large amount of less hydrated Cl bonds led to its lower zeta potential and less hydrophilic stage to show a better interaction with bubbles to reach a better flotation recovery.
(4) After adsorption of ODA, KCl(200) samples showed a weaker adhesion & adsorption force with KCl saturated solution than KCl (222), indicating its stronger interaction force with bubbles as well as easier floatability.

CRediT authorship contribution statement

Yuan Yuan: Writing – original draft, Methodology, Investigation, Conceptualization. **Weiquan Zhan:** Visualization, Software, Data curation. **Alejandro Lopéz Valdivieso:** Validation, Investigation. **Songliang Ma:** Formal analysis, Investigation, Methodology. **Yang Tian:** Resources, Data curation. **Hao Yi:** Project administration, Funding acquisition. **Guangfeng Dong:** Supervision, Validation. **Shaoxian Song:** Writing – review & editing, Supervision, Funding acquisition, Formal analysis. **Luis A. Cisternas:** Resources, Formal analysis. **Feifei Jia:** Visualization, Funding acquisition.

Declaration of competing interest

The authors declare that they have no known competing financial interests or personal relationships that could have appeared to influence the work reported in this paper.

Data availability

Data will be made available on request.

Acknowledgements

The authors gratefully appreciated the financial funds from the Key Research and Development Program of Xinjiang Province under projects No. 2022B01041. The work is financially supported by the National Key Research and Development Program of China (2022YFC2904004). This work was partially done by Luis A. Cisternas into visit at the Wuhan University of Technology, supported by MINEDUC-UA project, code ANT 22991. Yuan gratefully acknowledges the Consejo Nacional de Humanidades Ciencias y Tecnologías (CONAHCYT) of Mexico for offering her the scholarship under the grant No. 812586 during her Ph.D. studies.

References

[1] S. Titkov, Flotation of water-soluble mineral resources, Int. J. Miner. Process. 74 (2004) 107–113, https://doi.org/10.1016/J.MINPRO.2003.09.008.
[2] S. Ge, S.Y. Foong, N.L. Ma, R.K. Liew, W.A. Wan Mahari, C. Xia, P.N.Y. Yek, W. Peng, W.L. Nam, X.Y. Lim, C.M. Liew, C.C. Chong, C. Sonne, S.S. Lam, Vacuum pyrolysis incorporating microwave heating and base mixture modification: an integrated approach to transform biowaste into eco-friendly bioenergy products, Renew. Sust. Energ. Rev. 127 (2020) 109871, https://doi.org/10.1016/J.RSER.2020.109871.
[3] L.A. Pardo, W. Stühmer, The roles of K^+ channels in cancer, Nat. Rev. Cancer 14:1 (2013) 39–48, https://doi.org/10.1038/nrc3635.
[4] H. Gao, L. Xue, S. Xin, J.B. Goodenough, A high-energy-density potassium battery with a polymer-gel electrolyte and a polyaniline cathode, Angew. Chem. Int. Ed. 57 (2018) 5449–5453, https://doi.org/10.1002/ANIE.201802248.
[5] K. Xu, J. Li, X. Lv, J. Wu, X. Zhang, D. Xiao, J. Zhu, Superior piezoelectric properties in Potassium–Sodium niobate lead-free ceramics, Adv. Mater. 28 (2016) 8519–8523, https://doi.org/10.1002/ADMA.201601859.
[6] Q. Cao, X. Wang, J.D. Miller, F. Cheng, Y. Jiao, Bubble attachment time and FTIR analysis of water structure in the flotation of sylvite, bischofite and carnallite, Miner. Eng. 24 (2011) 108–114, https://doi.org/10.1016/J.MINENG.2010.10.006.
[7] H. Du, O. Ozdemir, X. Wang, F. Cheng, M.S. Celik, J.D. Miller, Flotation chemistry of soluble salt minerals: from ion hydration to colloid adsorption, Miner. Metall. Process. 31 (2014) 1–20, https://doi.org/10.1007/BF03402344/METRICS.
[8] C. Zörb, M. Senbayram, E. Peiter, Potassium in agriculture – status and perspectives, J. Plant Physiol. 171 (2014) 656–669, https://doi.org/10.1016/j.jplph.2013.08.008.
[9] S.K. Jena, B. Mohanty, G. Padhy, J. Sahu, S.K. Kandi, Potassium recovery from muscovite using NaCl-roasting followed by H2SO4-leaching, J. Cent. South Univ. 29 (2022) 1881–1894, https://doi.org/10.1007/S11771-022-5052-3/METRICS.
[10] E. Li, H. Liang, Z. Du, D. Li, F. Cheng, Adsorption process of Octadecylamine hydrochloride on KCl crystal surface in various salt saturated solutions: kinetics, isotherm model and thermodynamics properties, J. Mol. Liq. 221 (2016) 949–953, https://doi.org/10.1016/J.MOLLIQ.2016.06.050.
[11] X. Wu, Y. Chen, Z. Xing, C.W.K. Lam, S. Pang, W. Zhang, Z. Ju, Advanced carbon-based anodes for potassium-ion batteries, Adv. Energy Mater. 9 (2019), https://doi.org/10.1002/aenm.201900343.
[12] Z. Huang, C. Cheng, H. Zhong, L. Li, Z. Guo, X. Yu, G. He, H. Han, L. Deng, W. Fu, Flotation of sylvite from potash ore by using the Gemini surfactant as a novel flotation collector, Miner. Eng. 132 (2019) 22–26, https://doi.org/10.1016/J.MINENG.2018.11.055.
[13] Z. Huang, C. Cheng, Z. Liu, B. Feng, Y. Hu, W. Luo, G. He, X. Yu, W. Fu, Highly efficient potassium fertilizer production by using a gemini surfactant, Green Chem. 21 (2019) 1406–1411, https://doi.org/10.1039/C8GC03487G.
[14] J.S. Laskowski, From amine molecules adsorption to amine precipitate transport by bubbles: a potash ore flotation mechanism, Miner. Eng. 45 (2013) 170–179, https://doi.org/10.1016/j.mineng.2013.02.010.
[15] K. Sun, C.V. Nguyen, N.N. Nguyen, X. Ma, A.V. Nguyen, Crucial roles of ion-specific effects in the flotation of water-soluble KCl and NaCl crystals with fatty acid salts, J. Colloid Interface Sci. 636 (2023) 413–424, https://doi.org/10.1016/J.JCIS.2023.01.038.
[16] M. Hancer, M.S. Celik, J.D. Miller, The significance of interfacial water structure in soluble salt flotation systems, J. Colloid Interface Sci. 235 (2001) 150–161, https://doi.org/10.1006/JCIS.2000.7350.
[17] O. Ozdemir, H. Du, S.I. Karakashev, A.V. Nguyen, M.S. Celik, J.D. Miller, Understanding the role of ion interactions in soluble salt flotation with alkylammonium and alkylsulfate collectors, Adv. Colloid Interf. Sci. 163 (2011) 1–22, https://doi.org/10.1016/J.CIS.2011.01.003.
[18] K. Hanumantha Rao, K.S.E. Forssberg, Mechanism of fatty acid adsorption in salt-type mineral flotation, Miner. Eng. 4 (1991) 879–890, https://doi.org/10.1016/0892-6875(91)90071-3.
[19] Z. Liu, X. Zhong, Y. Liu, H. Rao, H. Wei, W. Hu, X. Nie, M. Liu, Adsorption and mechanism of Glycine on the Anatase with exposed (001) and (101) facets, Minerals 12 (2022) 798, https://doi.org/10.3390/MIN12070798.
[20] X. Gong, J. Yao, B. Yang, W. Yin, J. Guo, N. Song, Y. Wang, H. Sun, Activation–inhibition mechanism of diammonium hydrogen phosphate in flotation separation of brucite and calcite, J. Environ. Chem. Eng. 11 (2023) 110184, https://doi.org/10.1016/J.JECE.2023.110184.
[21] J. Yao, W. Yin, E. Gong, Depressing effect of fine hydrophilic particles on magnesite reverse flotation, Int. J. Miner. Process. 149 (2016) 84–93, https://doi.org/10.1016/J.MINPRO.2016.02.013.
[22] Y. Yuan, W. Zhan, F. Jia, S. Song, Multi-edged molybdenite achieved by thermal modification for enhancing Pb(II) adsorption in aqueous solutions, Chemosphere 251 (2020) 126369, https://doi.org/10.1016/j.chemosphere.2020.126369.
[23] W. Zhan, Y. Yuan, C. Liu, P. Chen, Y. Liang, Y. Wang, J.L. Arauz-Lara, F. Jia, Preparation and application of 0D, 2D and 3D molybdenite: a review, Miner. Mineral Mater. 1 (2022) 5, https://doi.org/10.20517/mmm.2022.04.
[24] M. Hirano, K. Shinjo, R. Kaneko, Y. Murata, Anisotropy of frictional forces in muscovite mica, Phys. Rev. Lett. 67 (1991) 2642, https://doi.org/10.1103/PhysRevLett.67.2642.

[25] W. Zhan, S. Yang, S. Bao, L. Ren, C. Liu, A novel insight of interaction mechanism of carboxymethyl cellulose with talc surface: a combined molecular dynamic simulation and DFT investigation, Appl. Clay Sci. 247 (2024) 107201, https://doi.org/10.1016/J.CLAY.2023.107201.
[26] G. Moos, C. Gahl, R. Fasel, M. Wolf, T. Hertel, Anisotropy of quasiparticle lifetimes and the role of disorder in graphite from ultrafast time-resolved photoemission spectroscopy, Phys. Rev. Lett. 87 (2001) 267402, https://doi.org/10.1103/PhysRevLett.87.267402.
[27] Y. Chen, X. Chen, Y. Peng, The effect of sodium hydrosulfide on molybdenite flotation as a depressant of copper sulfides, Miner. Eng. 148 (2020) 106203, https://doi.org/10.1016/J.MINENG.2020.106203.
[28] J. Yao, B. Yang, K. Chen, H. Sun, Z. Zhu, W. Yin, N. Song, Q. Sheng, Sodium tripolyphosphate as a selective depressant for separating magnesite from dolomite and its depression mechanism, Powder Technol. 382 (2021) 244–253, https://doi.org/10.1016/J.POWTEC.2020.12.040.
[29] G. Zhan, Z.C. Guo, Water leaching kinetics and recovery of potassium salt from sintering dust, Trans. Nonferrous Metals Soc. China 23 (2013) 3770–3779, https://doi.org/10.1016/S1003-6326(13)62928-3.
[30] E. Li, Z. Du, S. Yuan, F. Cheng, Low temperature molecular dynamic simulation of water structure at sylvite crystal surface in saturated solution, Miner. Eng. 83 (2015) 53–58, https://doi.org/10.1016/J.MINENG.2015.08.012.
[31] T. d'Almeida, Y.M. Gupta, Real-time X-ray diffraction measurements of the phase transition in KCl shocked along [100], Phys. Rev. Lett. 85 (2000) 330, https://doi.org/10.1103/PhysRevLett.85.330.
[32] A. Hossain, S. Roy, B.K. Dolui, Effects of thermodynamics on the solvation of amino acids in the pure and binary mixtures of solutions: a review, J. Mol. Liq. 232 (2017) 332–350, https://doi.org/10.1016/J.MOLLIQ.2017.02.080.
[33] Y. Yuan, W. Zhan, Y. Tian, A. López Valdivieso, H. Yi, S. Song, L.A. Cisternas, F. Jia, Novel strategy for improved sylvite flotation through controlled crystallization, Miner. Eng. 211 (2024) 108695, https://doi.org/10.1016/J.MINENG.2024.108695.
[34] L. Wang, Y. Xu, H. Chen, X. Song, New insights into octadecylamine-monoacid selective adsorption on KCl/NaCl surface: experimental and molecular dynamic simulation, Appl. Surf. Sci. 554 (2021) 149613, https://doi.org/10.1016/J.APSUSC.2021.149613.
[35] E. Li, Y. Zhang, Z. Du, D. Li, F. Cheng, Bubbles facilitate ODA adsorption and improve flotation recovery at low temperature during KCl flotation, Chem. Eng. Res. Des. 117 (2017) 557–563, https://doi.org/10.1016/J.CHERD.2016.11.016.
[36] L. Pastero, R. Cossio, D. Aquilano, {100} → {111} morphological change in KCl crystals grown from Pb^{2+}-doped aqueous solutions, CrystEngComm 17 (2015) 7844–7855, https://doi.org/10.1039/C5CE01425E.
[37] D.N. Krishnakumar, N.P. Rajesh, Growth and optical characterization of europium and cerium doped KCl single crystals by Czochralski method for Dosimetric applications, J. Electron. Mater. 48 (2019) 1629–1633, https://doi.org/10.1007/S11664-018-06863-3/METRICS.
[38] H. Qiu, Y. Zhang, W. Huang, J. Peng, J. Chen, L. Gao, M. Omran, N. Li, G. Chen, Sintering properties of tetragonal zirconia nanopowder preparation of the NaCl + KCl binary system by the sol-gel-flux method, ACS Sustain. Chem. Eng. 11 (2023) 1067–1077, https://doi.org/10.1021/ACSSUSCHEMENG.2C05908.
[39] Y. Zhong, J. Chen, M. Su, J. Han, Q. Wu, Solid–liquid equilibrium, crystal type, solid solubility and thermal stability studies of potassium ammonium chloride solid solution, Fluid Phase Equilib. 439 (2017) 24–30, https://doi.org/10.1016/j.fluid.2017.02.015.
[40] M. Shiehpour, S. Solgi, M.J. Tafreshi, M.S. Ghamsari, ZnO-doped KCl single crystal with enhanced UV emission lines, Appl. Phys. A 125 (2019) 531, https://doi.org/10.1007/s00339-019-2846-8.
[41] H. Wen, L. Liang, N. Xu, C. Liu, Multi-Functional Self-Cleaning Superhydrophobic Cotton Fabric as Photothermal-Reinforced Crude Oil Separator, Oil Skimmer and Underwater Oil Absorbent, Sep Purif Technol, 2024, p. 126258, https://doi.org/10.1016/j.seppur.2023.126258.
[42] K.-Y. Hwa, A. Ganguly, Effective monitoring of environmental hazardous drug moxifloxacin hydrochloride using silver selenide on octadecyl amine modified reduced graphene oxide composite, J. Environ. Chem. Eng. 12 (2024) 111694, https://doi.org/10.1016/J.JECE.2023.111694.
[43] T.V. Vu, A.A. Lavrentyev, B.V. Gabrelian, D.D. Vo, K.D. Pham, N.M. Denysyuk, L. I. Isaenko, A.Y. Tarasova, O.Y. Khyzhun, DFT study and XPS measurements elucidating the electronic and optical properties of KPb_2Cl_5, Opt. Mater. (Amst.) 102 (2020) 109793, https://doi.org/10.1016/j.optmat.2020.109793.
[44] J.D. Miller, S. Veeramasuneni, M.R. Yalamanchili, Recent contributions to the analysis of soluble salt flotation systems, Int. J. Miner. Process. 51 (1997) 111–123, https://doi.org/10.1016/S0301-7516(97)00037-9.
[45] E. Li, H. Liang, Z. Du, D. Li, F. Cheng, Adsorption process of Octadecylamine hydrochloride on KCl crystal surface in various salt saturated solutions: kinetics, isotherm model and thermodynamics properties, J. Mol. Liq. 221 (2016) 949–953, https://doi.org/10.1016/J.MOLLIQ.2016.06.050.